Supplementary Material: *Ab initio* Exchange-Correlation Free Energy of the Uniform Electron Gas at Warm Dense Matter conditions

Simon Groth[1], Tobias Dornheim[1], Travis Sjostrom[2], Fionn D. Malone[3], W.M.C. Foulkes[3], and Michael Bonitz[1]

[1]Institut für Theoretische Physik und Astrophysik, Christian-Albrechts-Universität zu Kiel, D-24098 Kiel, Germany
[2]Theoretical Division, Los Alamos National Laboratory, Los Alamos, New Mexico 87545, USA
[3]Department of Physics, Imperial College London, Exhibition Road, London SW7 2AZ, UK

A. Parametrization of the exchange correlation free energy

To represent the XC free energy for the spin-polarized and unpolarized case, $f^1_{\rm xc}(r_s,\theta)$ and $f^0_{\rm xc}(r_s,\theta)$, we use Padé formulae as introduced in Ref. [1]

$$f^\xi_{\rm xc}(r_s,\theta) = -\frac{1}{r_s}\frac{\omega_\xi a(\theta) + b^\xi(\theta)\sqrt{r_s} + c^\xi(\theta) r_s}{1 + d^\xi(\theta)\sqrt{r_s} + e^\xi(\theta) r_s} \;, \quad \text{(S.1)}$$

where $\theta = k_B T/E_F$, $r_s = \bar{r}/a_{\rm B}$, $\xi = (N^\uparrow - N^\downarrow)/(N^\uparrow + N^\downarrow)$, $\omega_0 = 1$ and $\omega_1 = 2^{1/3}$, and $a(\theta)$ denotes the Hartree-Fock limit as parametrized in Ref. [2]

$$a(\theta) = 0.610887 \tanh(\theta^{-1}) \times \frac{0.75 + 3.04363\theta^2 - 0.09227\theta^3 + 1.7035\theta^4}{1 + 8.31051\theta^2 + 5.1105\theta^4} \;.$$

The coefficients b, c, d, e are again Padé formulae with respect to temperature

$$\begin{aligned} b^\xi(\theta) &= \tanh\left(\frac{1}{\sqrt{\theta}}\right)\frac{b^\xi_1 + b^\xi_2\theta^2 + b^\xi_3\theta^4}{1 + b^\xi_4\theta^2 + b^\xi_5\theta^4} \\ c^\xi(\theta) &= \left[c^\xi_1 + c^\xi_2 \cdot \exp\left(-\theta^{-1}\right)\right] e^\xi(\theta) \\ d^\xi(\theta) &= \tanh\left(\frac{1}{\sqrt{\theta}}\right)\frac{d^\xi_1 + d^\xi_2\theta^2 + d^\xi_3\theta^4}{1 + d^\xi_4\theta^2 + d^\xi_5\theta^4} \\ e^\xi(\theta) &= \tanh\left(\frac{1}{\theta}\right)\frac{e^\xi_1 + e^\xi_2\theta^2 + e^\xi_3\theta^4}{1 + e^\xi_4\theta^2 + e^\xi_5\theta^4} \;. \end{aligned}$$

For completeness, we note that in Ref. [1], the parametrization from Eq. (S.1) was used for the interaction energy v instead of f_{xc}.

To parameterize $f_{\rm xc}$ as a function of the spin polarization $0 \le \xi \le 1$, we employ the ansatz [3]

$$f_{\rm xc}(r_s,\theta,\xi) = f^0_{\rm xc}(r_s,\theta^0) + \left[f^1_{\rm xc}(r_s,\theta^0\cdot 2^{-2/3}) - f^0_{\rm xc}(r_s,\theta^0)\right]\Phi(r_s,\theta^0,\xi) \;, \quad \text{(S.2)}$$

with $\theta^0 = \theta(1+\xi)^{2/3}$ and the interpolation function

$$\Phi(r_s,\theta,\xi) = \frac{(1+\xi)^{\alpha(r_s,\theta)} + (1-\xi)^{\alpha(r_s,\theta)} - 2}{2^{\alpha(r_s,\theta)} - 2}, \quad \text{(S.3)}$$
$$\alpha(r_s,\theta) = 2 - h(r_s)e^{-\theta\lambda(r_s,\theta)},$$
$$h(r_s) = \frac{2/3 + h_1 r_s}{1 + h_2 r_s}, \quad \lambda(r_s,\theta) = \lambda_1 + \lambda_2\theta r_s^{1/2} \;.$$

First, h_1 and h_2 are obtained by fitting $f_{\rm xc}(r_s,0,\xi)$ to the ground state data of Ref. [4] for $\xi = 0.34$ and $\xi = 0.66$. Subsequently, we use our extensive new QMC data set for $v^\xi(r_s,\theta)$ [107 data points for $\xi = 1/3$ and $\xi = 0.6$, see Tab. III] to determine λ_1 and λ_2. Interestingly, we find that the spin interpolation depends only very weakly on θ, i.e., λ_2 vanishes within the accuracy of the fit and, thus, we set $\lambda_2 = 0$.

All coefficients are listed in Tabs. I and II.

Table I: Parameters entering $f^\xi_{\rm xc}$ [cf. Eq. (S.1)], for $\xi = 0$ and $\xi = 1$.

	$\xi = 0$	$\xi = 1$
b_1	0.3436902	0.84987704
b_2	7.82159531356	3.04033012073
b_3	0.300483986662	0.0775730131248
b_4	15.8443467125	7.57703592489
b_5	$b_3(3/2)^{1/2}\omega_0\left(\frac{4}{9\pi}\right)^{-1/3}$	$b_3(3/2)^{1/2}\omega_1\left(\frac{4}{9\pi}\right)^{-1/3}$
c_1	0.8759442	0.91126873
c_2	-0.230130843551	-0.0307957123308
d_1	0.72700876	1.48658718
d_2	2.38264734144	4.92684905511
d_3	0.30221237251	0.0849387225179
d_4	4.39347718395	8.3269821188
d_5	0.729951339845	0.218864952126
e_1	0.25388214	0.27454097
e_2	0.815795138599	0.400994856555
e_3	0.0646844410481	2.88773194962
e_4	15.0984620477	6.33499237092
e_5	0.230761357474	24.823008753

Table II: Parameters entering the spin-interpolation function $\Phi(r_s,\theta,\xi)$ [cf. Eq. (S.3)].

h_1	-3.18747258
h_2	−7.74662802
λ_1	−1.85909536
λ_2	0

B. STLS

The static structure factor (SF) is found by the fluctuation-dissipation theorem as a sum over the Matsubara frequencies for the polarizabilities of the interacting

system as

$$S(\mathbf{k}) = \frac{-1}{\beta n} \sum_{l=-\infty}^{\infty} \frac{1}{v_k} \left(\frac{1}{\epsilon(\mathbf{k}, z_l)} - 1 \right) , \qquad \text{(S.4)}$$

with the particle density n, the Matsubara frequencies $z_l = 2\pi i l/\beta\hbar$, and the Fourier transform of the Coulomb potential $v_k = 4\pi/k^2$. Following [7], the Singwi-Tosi-Land-Sjölander (STLS) SF is computed from the dielectric function

$$\epsilon(\mathbf{k}, \omega) = 1 - \frac{v_k \chi_0(\mathbf{k}, \omega)}{1 + G(\mathbf{k}) v_k \chi_0(\mathbf{k}, \omega)} , \qquad \text{(S.5)}$$

with $\chi_0(\mathbf{q}, \omega)$ being the finite-temperature polarizability of the non-interacting UEG and G the static local field correction in STLS approximation

$$G(\mathbf{k}) = \frac{-1}{n} \int \frac{\mathrm{d}\mathbf{k}'}{(2\pi)^3} \frac{\mathbf{k} \cdot \mathbf{k}'}{k'^2} [S(\mathbf{k} - \mathbf{k}') - 1] . \qquad \text{(S.6)}$$

The STLS SF is then obtained via a self-consistent solution of Eq. (S.4), (S.5), and (S.6), which straight-forwardly allows to compute the corresponding interaction energy

$$v^{\mathrm{STLS}} = \frac{1}{\pi} \int_0^{\infty} \mathrm{d}k [S(k) - 1] . \qquad \text{(S.7)}$$

C. Finite-size correction of QMC data

Since QMC simulations are only feasible for a finite particle number N, it is necessary to extrapolate the results to the thermodynamic limit (TDL), $N \to \infty$. This is shown for the interaction energy in Fig. S1, where we plot v versus N^{-1} for the partially spin-polarized electron gas with $r_s = 1$, $\theta = 4$ and $\xi = 0.6$. The green crosses correspond to the original QMC data which, evidently, are strongly dependent on N. Therefore, we require a finite-size correction (FSC) ΔV_N that, in principle, should allow for the exact TDL using only a single QMC simulation:

$$v = \frac{V_N^{\mathrm{QMC}}}{N} + \frac{\Delta V_N}{N} . \qquad \text{(S.8)}$$

The first estimate for ΔV_N at finite T was proposed by Brown *et al.* [5] (BCDC). However, the results of adding the BCDC correction to the QMC data (the yellow asterisks in Fig. S1) are still not converged with N and, therefore, an improved approach is needed. In a recent Letter [6], we have shown that the main contribution to ΔV_N is a discretization error in the integration of the static structure factor $S(k)$ that can be accurately estimated by invoking the Singwi-Tosi-Land-Sjölander formalism [7] (hereafter denoted FS-STLS). The thus corrected data are depicted as the black squares. Evidently, simply adding the new FSC onto the bare QMC interaction energies immediately improves the accuracy by two orders of magnitude. The small residual error is due to an intrinsic N-dependence in the QMC results for $S(k)$ itself and can be removed by an additional extrapolation, the results of which is given by the red rhomb (for additional details see Refs. [6, 8]).

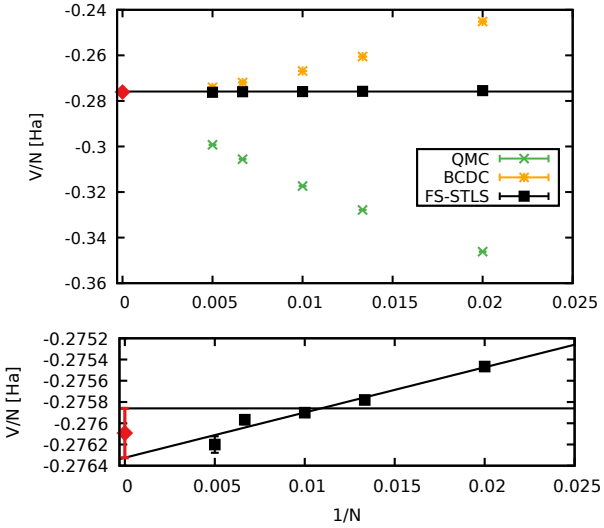

Figure S1: **Top:** Finite-size correction of the interaction energy for $\theta = 4$, $r_s = 1$, and $\xi = 0.6$. The green crosses correspond to the raw QMC data, the yellow asterisks are obtained by adding the FSC by Brown *et al.* [5] (BCDC), and the black squares by adding the recent FSC by Dornheim *et al.* [6] (FS-STLS). The red rhomb depicts the final result for the interaction energy obtained by an additional extrapolation of all residual errors. **Bottom:** Magnified part of the top panel.

D. QMC results for the XC energy

To calculate the finite-size correction for e_{xc} used in Fig. 2 of the main text, we first use the exact relationship between the exchange-correlation free energy and the potential energy:

$$f_{\mathrm{xc}} = \frac{1}{r_s^2} \int_0^{r_s} \mathrm{d}\bar{r}_s \bar{r}_s v(\bar{r}_s, \theta). \qquad \text{(S.9)}$$

This allows us to write the finite size correction for f_{xc} as

$$\Delta f_{\mathrm{xc}}(r_s, \theta) = \frac{1}{r_s^2} \int_0^{r_s} d\bar{r}_s \bar{r}_s \Delta v(\bar{r}_s, \theta), \qquad \text{(S.10)}$$

and, inserting this correction into Eq. (6) of the main text, we find

$$\Delta e_{\mathrm{xc}}(r_s, \theta) = \Delta f_{\mathrm{xc}}(r_s, \theta) - \theta \left(\frac{\partial \Delta f_{\mathrm{xc}}(r_s, \theta)}{\partial \theta} \right)_{r_s} . \qquad \text{(S.11)}$$

Thus, we first evaluate Δf_{xc}, before inserting this correction into Eq. (S.11), where the derivative term is evaluated numerically. More details of this procedure will be presented in a separate publication. For completeness, we mention that for $0.0625 \leq \theta \leq 0.5$ we have performed an additional twist-averaging of the QMC data as described in Refs. [9, 10].

E. Data tables

All interaction energies given in Table III have been obtained by performing QMC simulations for different N, adding the FS-STLS correction, and removing any residual errors by an additional extrapolation. Furthermore, Fig. S2 shows our entire data set and the resulting fit as well as a comparison to the KSDT parametrization [11] for both the potential energy v and the XC free energy f_{xc}.

Table III: Finite-size corrected potential energy from finite temperature QMC simulations.

ξ	θ	r_s	$v \cdot r_s$	$\delta v \cdot r_s$
0	8.00	20.0	−0.604 414	0.000 094
0	4.00	20.0	−0.677 788	0.000 041
0	2.00	20.0	−0.726 928	0.000 022
0	1.00	20.0	−0.752 044	0.000 020
0	0.75	20.0	−0.752 948	0.000 050
0	0.75	10.0	−0.710 858	0.000 052
0	0.75	4.0	−0.637 257	0.000 267
0	0.75	2.0	−0.570 146	0.000 821
0	0.75	1.0	−0.503 977	0.002 348
0	0.75	0.5	−0.443 621	0.000 918
0	0.75	0.3	−0.403 418	0.000 537
0	0.75	0.1	−0.335 412	0.000 230
0	0.50	20.0	−0.756 936	0.000 184
1/3	8.00	20.0	−0.580 376	0.000 120
1/3	8.00	10.0	−0.484 172	0.000 294
1/3	8.00	6.0	−0.411 857	0.000 449
1/3	8.00	4.0	−0.357 279	0.000 398
1/3	8.00	2.0	−0.274 122	0.000 604
1/3	8.00	1.0	−0.209 039	0.000 126
1/3	8.00	0.5	−0.158 207	0.000 089
1/3	8.00	0.3	−0.129 225	0.000 092
1/3	8.00	0.1	−0.085 583	0.000 081
1/3	4.00	20.0	−0.659 796	0.000 055
1/3	4.00	10.0	−0.575 249	0.000 103
1/3	4.00	6.0	−0.506 857	0.000 226
1/3	4.00	4.0	−0.451 411	0.000 177
1/3	4.00	2.0	−0.362 040	0.000 303
1/3	4.00	1.0	−0.285 290	0.000 262
1/3	4.00	0.5	−0.222 982	0.000 083
1/3	4.00	0.3	−0.186 455	0.000 060
1/3	4.00	0.1	−0.129 779	0.000 045
1/3	2.00	20.0	−0.716 060	0.000 022
1/3	2.00	10.0	−0.648 594	0.000 050
1/3	2.00	6.0	−0.589 913	0.000 100
1/3	2.00	4.0	−0.540 310	0.000 082
1/3	2.00	2.0	−0.453 908	0.000 271
1/3	2.00	1.0	−0.373 593	0.000 539
1/3	2.00	0.5	−0.305 016	0.000 481
1/3	2.00	0.3	−0.262 926	0.000 177
1/3	2.00	0.1	−0.195 205	0.000 098
1/3	1.00	20.0	−0.746 370	0.000 016
1/3	1.00	10.0	−0.695 351	0.000 060
1/3	1.00	6.0	−0.649 843	0.000 125
1/3	1.00	4.0	−0.609 682	0.000 275
1/3	1.00	2.0	−0.533 920	0.000 330
1/3	1.00	1.0	−0.461 622	0.000 655
1/3	1.00	0.5	−0.395 233	0.000 664
1/3	1.00	0.3	−0.353 105	0.000 245
1/3	1.00	0.1	−0.282 035	0.000 135
1/3	0.75	20.0	−0.752 258	0.000 024
1/3	0.75	10.0	−0.706 095	0.000 112
1/3	0.75	6.0	−0.665 854	0.000 305
1/3	0.75	4.0	−0.629 244	0.000 194
1/3	0.75	2.0	−0.561 332	0.000 627
1/3	0.75	1.0	−0.491 727	0.001 049
1/3	0.75	0.5	−0.430 284	0.000 834
1/3	0.75	0.3	−0.389 745	0.000 636
1/3	0.75	0.1	−0.321 438	0.000 135
1/3	0.50	20.0	−0.756 208	0.000 265
1/3	0.50	10.0	−0.717 354	0.001 175
1/3	0.50	6.0	−0.675 084	0.001 677
1/3	0.50	4.0	−0.647 064	0.000 515
1/3	0.50	2.0	−0.586 194	0.002 044
1/3	0.50	1.0	−0.525 908	0.002 428
1/3	0.50	0.5	−0.472 038	0.001 061
1/3	0.50	0.3	−0.436 211	0.000 508
1/3	0.50	0.1	−0.374 860	0.000 130
0.6	8.00	20.0	−0.564 678	0.000 130
0.6	8.00	10.0	−0.467 239	0.000 265
0.6	8.00	6.0	−0.396 677	0.000 580
0.6	8.00	4.0	−0.342 476	0.000 305
0.6	8.00	2.0	−0.262 646	0.000 269
0.6	8.00	1.0	−0.200 652	0.000 122
0.6	8.00	0.5	−0.152 350	0.000 110
0.6	8.00	0.3	−0.124 913	0.000 116
0.6	8.00	0.1	−0.084 291	0.000 419
0.6	4.00	20.0	−0.647 332	0.000 054
0.6	4.00	10.0	−0.560 424	0.000 094
0.6	4.00	6.0	−0.491 593	0.000 175
0.6	4.00	4.0	−0.437 054	0.000 291
0.6	4.00	2.0	−0.349 670	0.000 316
0.6	4.00	1.0	−0.276 092	0.000 232
0.6	4.00	0.5	−0.216 875	0.000 074
0.6	4.00	0.3	−0.182 187	0.000 253
0.6	4.00	0.1	−0.128 691	0.000 238
0.6	2.00	20.0	−0.708 140	0.000 025
0.6	2.00	10.0	−0.638 071	0.000 060
0.6	2.00	6.0	−0.578 400	0.000 092
0.6	2.00	4.0	−0.528 572	0.000 173
0.6	2.00	2.0	−0.443 764	0.000 460
0.6	2.00	1.0	−0.365 352	0.000 547
0.6	2.00	0.5	−0.300 452	0.000 180
0.6	2.00	0.3	−0.260 321	0.000 110
0.6	2.00	0.1	−0.196 527	0.000 285
0.6	1.00	20.0	−0.742 986	0.000 015
0.6	1.00	10.0	−0.690 110	0.000 058
0.6	1.00	6.0	−0.643 421	0.000 551
0.6	1.00	4.0	−0.602 959	0.000 130
0.6	1.00	2.0	−0.529 821	0.000 309
0.6	1.00	1.0	−0.458 146	0.000 503
0.6	1.00	0.5	−0.395 825	0.001 016
0.6	1.00	0.3	−0.354 692	0.000 300
0.6	1.00	0.1	−0.287 919	0.000 131
0.6	0.75	20.0	−0.750 356	0.000 017
0.6	0.75	10.0	−0.703 143	0.000 485
0.6	0.75	6.0	−0.661 680	0.000 177
0.6	0.75	4.0	−0.624 412	0.000 407
0.6	0.75	2.0	−0.559 316	0.000 421
0.6	0.75	1.0	−0.491 014	0.002 800
0.6	0.75	0.5	−0.433 163	0.000 603
0.6	0.75	0.3	−0.394 409	0.000 533
0.6	0.75	0.1	−0.329 384	0.000 093
0.6	0.50	20.0	−0.755 894	0.000 093
0.6	0.50	10.0	−0.714 236	0.001 111
0.6	0.50	6.0	−0.678 234	0.000 645
0.6	0.50	2.0	−0.589 876	0.000 620

ξ	θ	r_s	$v \cdot r_s$	$\delta v \cdot r_s$
0.6	0.50	1.0	−0.531 667	0.000 524
0.6	0.50	0.5	−0.480 832	0.001 670
0.6	0.50	0.3	−0.445 028	0.000 740
0.6	0.50	0.1	−0.386 802	0.000 116
1	8.00	0.1	−0.086 133	0.000 027
1	8.00	0.3	−0.124 165	0.000 047
1	8.00	0.5	−0.149 504	0.000 047
1	8.00	1.0	−0.194 203	0.000 066
1	8.00	2.0	−0.252 452	0.000 303
1	8.00	4.0	−0.327 037	0.000 261
1	8.00	6.0	−0.378 252	0.000 426
1	8.00	8.0	−0.417 303	0.000 404
1	8.00	10.0	−0.448 115	0.000 486
1	8.00	20.0	−0.544 914	0.000 177
1	4.00	0.1	−0.135 554	0.000 036
1	4.00	0.3	−0.184 652	0.000 070
1	4.00	0.5	−0.216 525	0.000 082
1	4.00	1.0	−0.270 858	0.000 615
1	4.00	2.0	−0.339 262	0.000 172
1	4.00	4.0	−0.421 696	0.000 232
1	4.00	6.0	−0.474 381	0.000 083
1	4.00	8.0	−0.512 738	0.000 137
1	4.00	10.0	−0.542 639	0.000 076
1	4.00	20.0	−0.631 370	0.000 078
1	2.00	0.1	−0.211 965	0.000 104
1	2.00	0.3	−0.269 952	0.000 134
1	2.00	0.5	−0.306 107	0.000 140
1	2.00	1.0	−0.365 728	0.000 374
1	2.00	2.0	−0.436 766	0.000 385
1	2.00	4.0	−0.516 652	0.000 170
1	2.00	6.0	−0.564 960	0.000 167
1	2.00	8.0	−0.599 070	0.000 084
1	2.00	10.0	−0.624 687	0.000 078
1	2.00	20.0	−0.697 464	0.000 038
1	1.00	0.1	−0.318 360	0.000 133
1	1.00	0.3	−0.376 986	0.000 132
1	1.00	0.5	−0.412 091	0.000 138
1	1.00	1.0	−0.466 598	0.000 999
1	1.00	2.0	−0.529 651	0.000 478
1	1.00	4.0	−0.597 449	0.000 123
1	1.00	6.0	−0.636 542	0.000 086
1	1.00	8.0	−0.663 264	0.000 075
1	1.00	10.0	−0.683 287	0.000 074
1	1.00	20.0	−0.738 042	0.000 021
1	0.75	0.1	−0.368 039	0.000 107
1	0.75	0.3	−0.423 521	0.000 149
1	0.75	0.5	−0.456 112	0.000 261
1	0.75	1.0	−0.506 379	0.000 646
1	0.75	2.0	−0.564 127	0.000 187
1	0.75	4.0	−0.624 104	0.000 543
1	0.75	6.0	−0.658 458	0.000 136
1	0.75	10.0	−0.699 291	0.000 053
1	0.75	20.0	−0.747 552	0.000 012
1	0.50	0.1	−0.436 852	0.000 150
1	0.50	0.3	−0.484 687	0.000 114
1	0.50	0.5	−0.512 677	0.000 305
1	0.50	1.0	−0.553 536	0.001 915
1	0.50	2.0	−0.600 776	0.002 929
1	0.50	4.0	−0.651 476	0.000 679
1	0.50	6.0	−0.680 010	0.001 349
1	0.50	8.0	−0.699 106	0.000 564
1	0.50	10.0	−0.713 698	0.000 201
1	0.50	20.0	−0.755 328	0.000 037

[1] S. Ichimaru, H. Iyetomi, and S. Tanaka, Statistical physics of dense plasmas: Thermodynamics, transport coefficients and dynamic correlations, *Physics Reports* **149**, 91 (1987)

[2] F. Perrot and M.W.C. Dharma-wardana, Exchange and correlation potentials for electron-ion systems at finite temperatures, *Phys. Rev. A* **30**, 2619 (1984)

[3] F. Perrot and M.W.C. Dharma-wardana, Spin-polarized electron liquid at arbitrary temperatures: Exchange-correlation energies, electron-distribution functions, and the static response functions, *Phys. Rev. B* **62**, 16536 (2000)

[4] G.G. Spink, R.J. Needs, and N.D. Drummond, Quantum Monte Carlo Study of the Three-Dimensional Spin-Polarized Homogeneous Electron Gas, *Phys. Rev. B* **88**, 085121 (2013)

[5] E.W. Brown, B.K. Clark, J.L. DuBois and D.M. Ceperley, Path-Integral Monte Carlo Simulation of the Warm Dense Homogeneous Electron Gas, *Phys. Rev. Lett.* **110**, 146405 (2013)

[6] T. Dornheim, S. Groth, T. Sjostrom, F.D. Malone, W.M.C. Foulkes, and M. Bonitz, *Ab Initio* Quantum Monte Carlo Simulation of the Warm Dense Electron Gas in the Thermodynamic Limit, *Phys. Rev. Lett.* **117**, 156403 (2016)

[7] S. Tanaka and S. Ichimaru, Thermodynamics and Correlational Properties of Finite-Temperature Electron Liquids in the Singwi-Tosi-Land-Sjölander Approximation, *J. Phys. Soc. Jpn.* **55**, 2278-2289 (1986)

[8] T. Dornheim, S. Groth, F.D. Malone, T. Schoof, T. Sjostrom, W.M.C. Foulkes, and M. Bonitz, *Ab Initio* Quantum Monte Carlo Simulation of the Warm Dense Electron Gas, *Physics of Plasmas* **24**, 056303 (2017)

[9] N.D. Drummond, R.J. Needs, A. Sorouri and W.M.C. Foulkes, Finite-size errors in continuum quantum Monte Carlo calculations, *Phys. Rev. B* **78**, 125106 (2008)

[10] C. Lin, F.H. Zong and D.M. Ceperley, Twist-averaged boundary conditions in continuum quantum Monte Carlo algorithms, *Phys. Rev. E* **64**, 016702 (2001)

[11] V.V. Karasiev, T. Sjostrom, J. Dufty and S.B. Trickey, Accurate Homogeneous Electron Gas Exchange-Correlation Free Energy for Local Spin-Density Calculations, *Phys. Rev. Lett.* **112**, 076403 (2014)

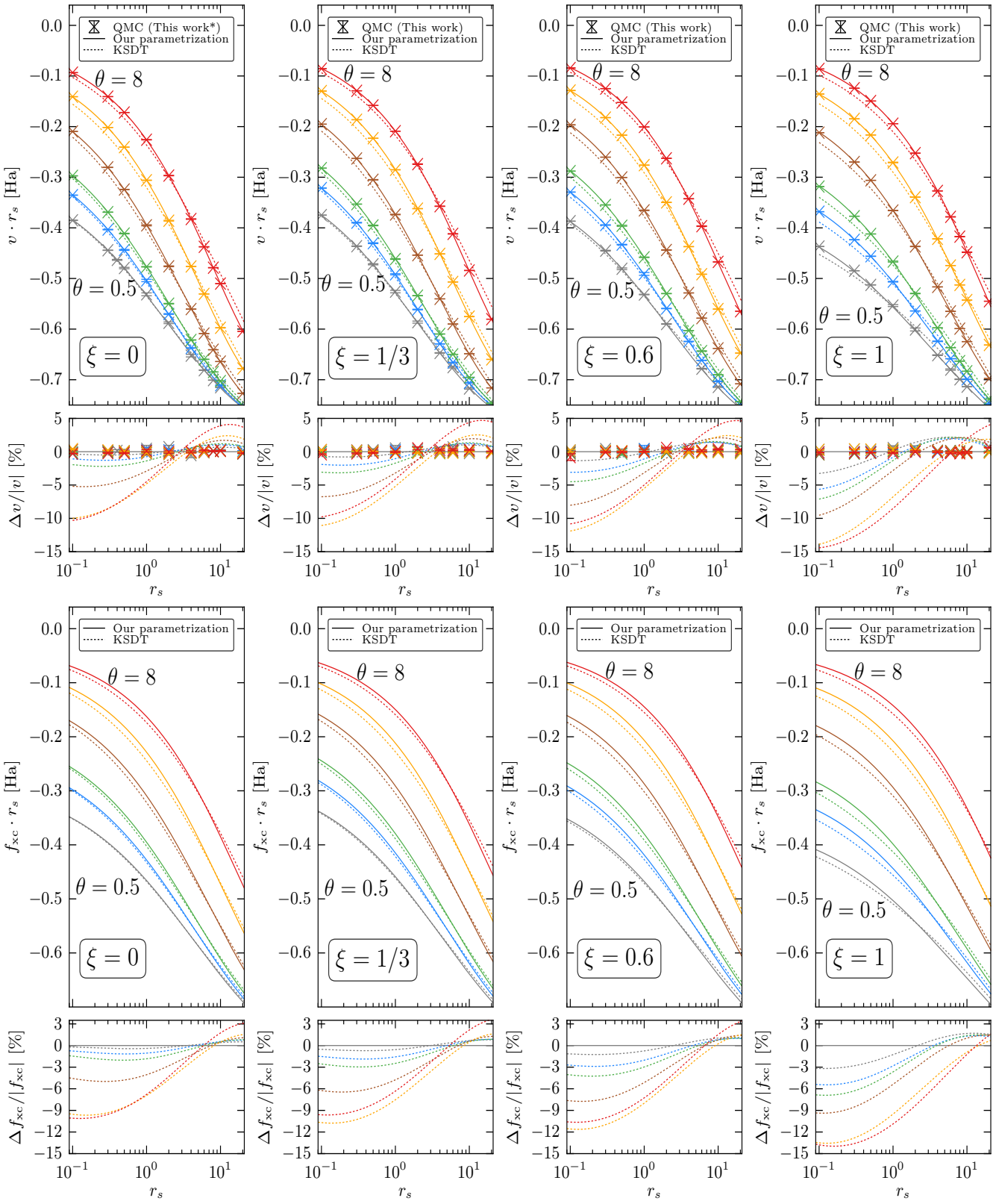

Figure S2: **Top row:** Upper panel: Density dependence of the potential energy for different temperatures (top to bottom: $\theta = 8, 4, 2, 1, 0.75, 0.5$). Crosses: new QMC data of this work for $\xi = 1/3, 0.6$, and 1. For $\xi = 0$, the data from Ref. [6] are plotted (indicated by the $*$ in the legend) in addition to the new data points for $\theta = 0.75$ and also for $r_s = 20$. Solid line: Our parametrization ($r_s - \theta - \xi$-fit to the QMC data). Dashed line: KSDT parametrization [11]. Lower panel: Deviation of the QMC data (crosses) and the KSDT parametrization (dashed line) from our parametrization. **Bottom row:** Upper panel: Density dependence of the exchange-correlation free energy for different temperatures (top to bottom: $\theta = 8, 4, 2, 1, 0.75, 0.5$). Solid line: Our parametrization. Dashed line: KSDT prametrization. Lower panel: Deviation of KSDT from our parametrization.